A Letters Journal Exploring the Frontiers of Physics

May 2007

EPL, **78** (2007) 40004
doi: 10.1209/0295-5075/78/40004

www.epljournal.org

Observation of twin beam correlations and quadrature entanglement by frequency doubling in a two-port resonator

O.-K. Lim, B. Boland and M. Saffman

Department of Physics, University of Wisconsin - 1150 University Avenue, Madison, WI 53706, USA

received 12 February 2007; accepted in final form 10 April 2007
published online 9 May 2007

PACS 03.67.Mn – Entanglement production, characterization and manipulation
PACS 42.50.Dv – Nonclassical states of the electromagnetic field, including entangled photon states; quantum state engineering and measurements
PACS 42.65.Ky – Frequency conversion; harmonic generation, including higher-order harmonic generation

Abstract – We demonstrate production of short wavelength beams with nonclassical intensity correlations and quadrature entanglement using second harmonic generation in a nonlinear resonator with two output ports. The two output beams at the harmonic frequency have no direct interaction but are both nonlinearly coupled to a common pump beam. The nonlinear coupling produces amplitude and phase correlations between the beams which results in quadrature entanglement. The output beams at $\lambda = 428.5\,\mathrm{nm}$ are shown to exhibit 0.6 dB of amplitude quadrature squeezing, 0.9 dB of nonclassical intensity correlations, and 0.3 dB of entanglement using about 30 mW of pump power.

Continuous light beams that exhibit nonclassical statistics and entanglement are of interest in studies of quantum fields [1] and for a number of applications that include precision measurements [2], writing subwavelength spatial structures [3], and as resources for quantum information and communication protocols [4]. The most successful and widely used approach to generating continuous variable entangled light beams employs parametric downconversion in crystals with a quadratic nonlinearity [5]. At the microscopic level non-classical correlations and entanglement arise due to the possibility of converting a single high frequency photon at 2ω into a pair of entangled lower frequency photons at ω [6].

In order to experimentally generate entangled beams with carrier frequency ω, one typically starts with a coherent source at ω which is frequency doubled to 2ω. The light at 2ω is then used to drive a downconversion process to generate nonclassical light at frequency ω. These multiple steps add to the complexity of the experimental arrangement and limit the possibility of generating entangled light at short wavelengths. In this letter we demonstrate for the first time that nonclassical intensity correlations, as well as quadrature entangled beams, can be generated directly by frequency upconversion. In this way a coherent source at frequency ω produces quantum correlated beams at frequency 2ω which may be important for applications such as quantum lithography [3] which will benefit from short wavelength entanglement.

Consider the interaction geometry shown in fig. 1 where a beam of frequency ω pumps a resonator that has two exit ports for the second harmonic beams at frequency 2ω. The cavity mirrors are assumed perfectly transmitting for the harmonic beams which are generated in a single pass of the intracavity pump field through the nonlinear crystal. It is well known that second harmonic generation (SHG) results in squeezing of the fundamental and harmonic beams [7]. The generation of multibeam correlations in second harmonic generation is less well studied than in the case of parametric downconversion. Calculations have demonstrated the existence of correlations between the fundamental and harmonic fields [8] including entanglement between the fundamental and harmonic fields [9] and entanglement in type-II SHG in the fundamental fields alone [10]. The possibility of nonclassical spatial correlations in either the fundamental or harmonic fields alone [11] and of entanglement in the fundamental field [12] has also been shown in models that include diffraction. Here we consider a situation where there are two harmonic output beams which share the same intracavity pump field. The common pump field couples the output beams, and our recent analysis of this interaction geometry [13] reveals that the two outputs exhibit nonclassical

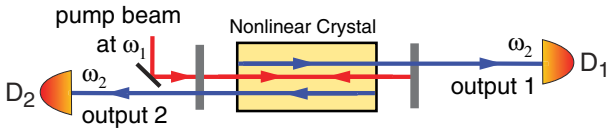

Fig. 1: (Color online) Conceptual schematic for generation of intensity correlations and quadrature entanglement by SHG in a two-port resonator. The output beams leaving the resonator are quadrature entangled without further interactions.

intensity correlations, as well as quadrature entanglement. We emphasize that the strength of the entanglement generated in the geometry of fig. 1 depends on the buildup of amplitude and phase correlations between the output beams due to the fact that they are both nonlinearly coupled to the common intracavity pump field at ω. The outputs 1 and 2 are entangled upon leaving the cavity even though there is no place where linear interference between the beams occurs. This is fundamentally different than entanglement generation based on combining two independently squeezed beams on a beamsplitter [14].

Nonclassical intensity correlations can be demonstrated by comparing the fluctuations of the sum and difference of the photocurrents generated by the output beams. We combine the detector outputs to form the quantities $I_{d/s} = I_1 \mp gI_2$, where g is an electronic scale factor. Calculations that account for the propagation of fluctuations in the two-ported cavity [13] show that with optimal choice of the scale factor g the variance of the sum and difference photocurrent fluctuations is

$$(\Delta|i_{d/s}|)^2_{\rm norm} = S_X \pm \frac{1}{2}C_X. \qquad (1)$$

Here S_X is the amplitude quadrature noise spectrum of each harmonic output, C_X is the correlation coefficient of the amplitude quadratures at the two output ports, and we have simplified the more general expression given in ref. [13] to the case where the two output beams have identical squeezing spectra. It can be shown that the difference photocurrent is extremely close to the shot noise level while the noise of the sum photocurrent is suppressed below the shot noise. The reduced noise in the sum photocurrent arises from the amplitude squeezing of each beam and from the quantum correlations of the beams generated by the two-port cavity. As we demonstrate experimentally below the noise reduction of the intensity sum is greater than that due to the amplitude squeezing of each beam alone which proves the role played by the shared intracavity pump beam in creating a nonzero correlation C_X.

Calculations show that the output beams are entangled according to the Duan *et al.* inseparability criteria [15] and exhibit EPR correlations for sufficiently high pump power. It can be shown that the beams are inseparable when the inequality [13] $V = \frac{1}{4}(2S_X + 2S_Y + C_X - C_Y) < 1$ is satisfied where S_Y is the phase quadrature noise spectrum of each beam, and C_Y is the phase quadrature correlation coefficient of the beams. We see that verifying

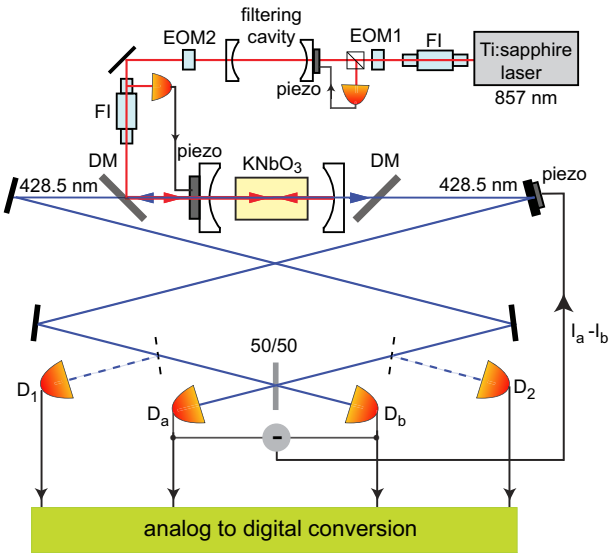

Fig. 2: (Color online) Experimental setup for entanglement generation with a dual-ported resonator. FI = Faraday isolator, EOM = electrooptic modulator, DM = dichroic mirror. By inserting the mirrors shown with dashed lines detectors D_1, D_2 are used to verify intensity correlations. Detectors D_a, D_b are used for entanglement measurements. All detectors are Hamamatsu S3590-19 with quantum efficiency of $\eta = 0.96$ at 429 nm.

the presence of quadrature entanglement between the beams is technically more difficult than intensity correlation measurements since it requires measuring both the amplitude and phase fluctuations. As the beams generated by SHG have a nonzero mean amplitude, measurement of the phase quadrature using a strong local oscillator is inconvenient due to detector saturation. Instead, we use an entanglement witness demonstrated by Glöckl *et al.* [16,17] which allows us to verify quadrature entanglement using only intensity measurements. The beams are combined on a 50/50 beamsplitter with a $\pi/2$ phase difference and the intensity fluctuations of the output beams are measured. The variances of the sum and difference photocurrents after the beamsplitter are $(\Delta|i_+|)^2 = 2S_X + C_X$ and $(\Delta|i_-|)^2 = 2S_Y - C_Y$. The inseparability criterion can then be expressed as

$$(\Delta|i_+|)^2 + (\Delta|i_-|)^2 < 4 \qquad (2)$$

which can be verified on the basis of intensity measurements alone.

We have observed nonclassical beam correlations in a dual-ported resonator as shown in fig. 2. The experiment uses an Ar-ion pumped Ti:Sa laser operating at 857 nm which is frequency doubled with a $KNbO_3$ crystal in a confocal linear resonator. In order to suppress low frequency intensity noise the beam from the Ti:Sa laser was locked to a mode-cleaning cavity with linewidth 1.5 MHz (FWHM) using a standard radio frequency (rf) modulation technique [18]. The beam was then mode-matched to a dual ported linear cavity with two plano-concave mirrors with radius of curvature $R = 10$ mm

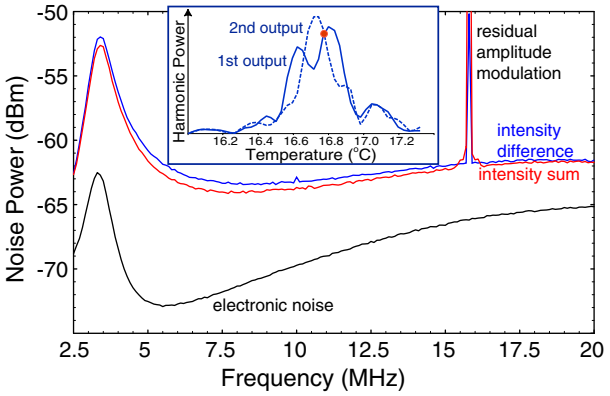

Fig. 3: (Color online) Spectra of the intensity noise for the intensity difference and sum of the two second harmonic fields. The broad response peak centered at 3.5 MHz is due to the filtering circuit used for AC-coupling of the photocurrent. The sharp peak at 15.8 MHz is due to residual modulation from the rf cavity lock. The data was acquired in 80 ms and the effective numerical resolution bandwidth is 100 kHz. The inset shows measured phase matching curves for the first (solid line) and second (dashed line) outputs from the dual-ported resonator at $P_{\rm pump} = 31\,{\rm mW}$. The phase mismatch parameter $\Delta kL = \pi$ corresponds to a temperature change of about 0.25 °C.

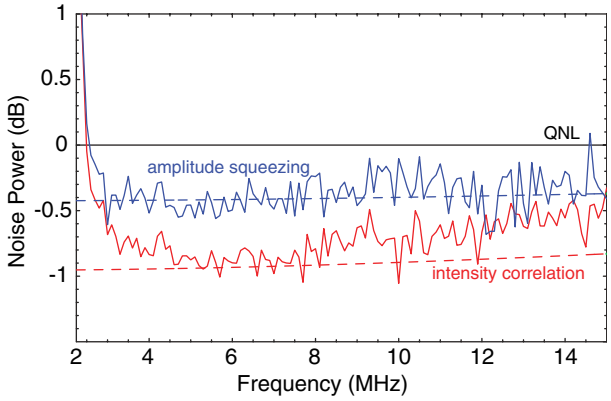

Fig. 4: (Color online) Noise spectra of the intensity sum (red curve) and amplitude squeezing of the first harmonic output measured at an output power of 9 mW (blue curve). The amplitude squeezing of the second harmonic output agrees with the first output to ±0.1 dB. The shot noise reference level (QNL) was determined for the amplitude squeezing measurements using the difference of two detectors placed in one output port. The theory curves for the intensity sum and squeezing (dashed lines) were calculated using the cavity parameters given in the text and with a single pass conversion efficiency of $E_{NL} = 0.0059\,{\rm W}^{-1}$ which was determined from the measured harmonic output power. The experimental data were corrected for electronic noise, but no correction was made for detector quantum efficiency and optical losses between cavity and detectors estimated to be 5%.

containing a 1 cm long a-cut $KNbO_3$ crystal with anti-reflection coated ends. The input mirror had $T_{857\,\rm nm} = 4\%$ and $R_{428\,\rm nm} < 5\%$. The output mirror had $R_{857\,\rm nm} > 99\%$ and $R_{428\,\rm nm} < 5\%$. Hence, only the fundamental field was resonant in the cavity. The separation of the mirrors was set to 15.6 mm for confocal operation and the low power cavity finesse was measured to be 120. The cavity linewidth (FWHM) was 43 MHz. Using the measured finesse and the input coupler transmission, the roundtrip intracavity loss was calculated to be about 1.1%.

Phase matching was controlled by varying the temperature of the crystal to produce two counter-propagating bright blue beams of wavelength 428.5 nm. The temperature tuning curves for the two harmonic outputs are shown in the inset of fig. 3. The second output (counterpropagating to the incident pump beam) resembles the standard SHG phase matching curve for propagation without a cavity while the first output (copropagating with the incident pump beam) shows two distinct maxima. We believe the shape of the curves and the difference in optimal phase matching temperatures is due to a small but finite reflectivity of the cavity mirrors at the harmonic wavelength which changes the intracavity boundary conditions. A related sensitive dependence of the relative phase of the fundamental and harmonic fields on cavity parameters was noted in our earlier studies of self-pulsing in SHG [19]. The experiments described below were performed using a crystal temperature of about 16.8 °C which equalizes the output powers as indicated in the figure. In this case we expect the theoretical model used in ref. [13] to provide an accurate description of the experiment.

The SHG cavity was locked to be resonant with the laser frequency ω to generate stable harmonic outputs in both directions. At $P_{\rm pump} = 34\,{\rm mW}$ incident on the cavity, 8 mW of 428.5 nm light was generated in each output beam. By inserting movable mirrors in the output beams detectors D_1 and D_2 were used to measure the intensities of the two outputs as shown in the inset of fig. 3. The detector outputs were amplified and then recorded with a dual channel analog to digital converter (CompuScope 14200, sampling frequency = 200 Msamples/s, 14 bit data). The noise power spectra of the difference and sum of the photocurrents were computed using a standard Fourier transform technique.

The measured noise spectra of the intensity sum and difference correlations with $g = 1$ are given in figs. 3 and 4. The shot noise limit (QNL) for the intensity correlation is given by the noise spectrum of the intensity difference of the two output ports. The maximum non-classical intensity correlation (corrected for electronic noise) was -0.90 ± 0.15 dB at a noise frequency of 6 MHz. The experimentally measured and theoretical noise reduction calculated from eq. (1) agreed to better than 5% over the range of about 4–8 MHz. The theoretical curves show only a weak frequency dependence since the cavity bandwidth is large compared to the frequency range shown in the figures. At lower frequencies the effect was masked by technical laser noise and at higher frequencies roll-off in the detector response reduced the magnitude of the observed effect. The amplitude noise of one of the output beams is shown by the blue (on-line) line. We see that the noise reduction in the intensity sum clearly exceeds the

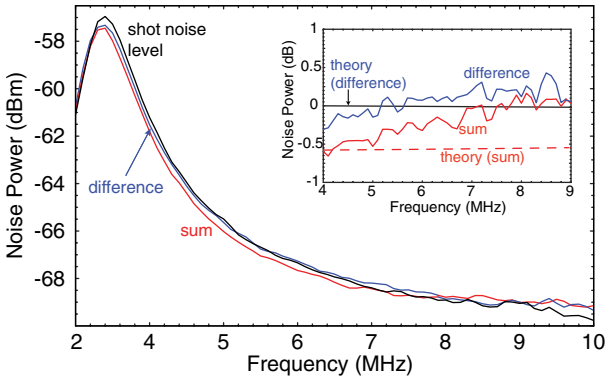

Fig. 5: (Color online) Noise spectra measured by detectors D_a, D_b corrected for electronic noise. The intensity sum which gives the amplitude quadrature (red curve) and intensity difference which gives the phase quadrature (blue curve) are shown with the shot noise level $(\Delta|i_{12}|)^2$ (black curve). The inset shows the sum and difference spectra relative to the measured shot noise level together with the corresponding theory curves calculated with the same parameters as in fig. 4 but with $P_{\rm pump} = 23\,$mW. The spectra in figs. 5, 6 were calculated with a numerical resolution bandwidth of 200 kHz.

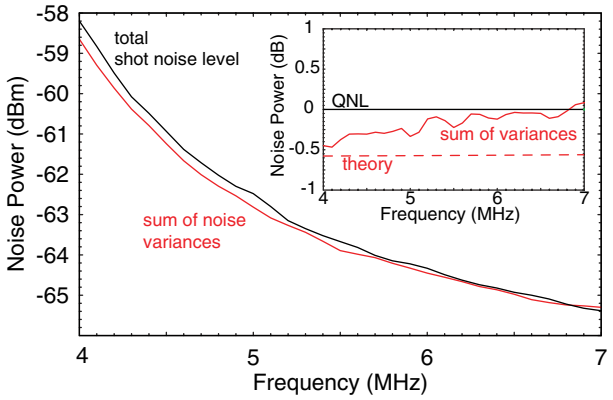

Fig. 6: (Color online) Noise power of the sum of noise variances (red curve) together with the quantum noise limit $2(\Delta|i_{12}|)^2$ (black curve). The inset shows the difference of the two curves together with the theoretical result using the same parameters as in fig. 5.

amplitude squeezing of the individual beams which establishes the presence of the additional correlation C_X between the beams created in the SHG cavity.

In order to verify entanglement of the second harmonic beams we measured the sum and difference intensity noise after mixing on the 50/50 beamsplitter shown in fig. 2. The first mirror on the right side of the SHG cavity was mounted on a piezo to allow active correction of the path length difference between the two interfering arms. The photocurrents from D_a and D_b were recorded with a dual channel analog to digital converter and analyzed in the same way as for the measurements of the intensity correlations. In this configuration the difference of the photocurrents from D_1 and D_2 gives the corresponding shot noise level of the two entangled beams [17]. The shot noise level was calculated as $(\Delta|i_{12}|)^2 = (\Delta|i_1 - 0.95 i_2|)^2$, where the gain factor of 0.95 was used to account for a small difference in signal level in the two arms. We emphasize that introduction of this factor lowered the shot noise reference level and only reduced the magnitude of the non-classical effects we describe below.

The results of the measurements for $P_{\rm pump} = 23\,$mW and 3.3 mW of harmonic power on each output are shown in fig. 5. At 5 MHz, the sum variance was $(0.50 \pm 0.15)\,$dB below the shot noise level and the normalized noise variance (amplitude correlation) was $(\Delta|i_+|)^2 = 1.78 \pm 0.07$. The difference variance was $(0.10 \pm 0.15)\,$dB below the shot noise level giving a normalized noise variance (phase correlation) of $(\Delta|i_-|)^2 = 1.95 \pm 0.07$. We find

$$\begin{aligned}(\Delta|i_+|)^2 + (\Delta|i_-|)^2 &= (1.78 \pm 0.07) + (1.95 \pm 0.07) \\ &= 3.73 \pm 0.14 < 4,\end{aligned}$$

which satisfies the inseparability criterion given in eq. (2). Expressed in dB the entanglement signature is $10\log_{10}(3.73/4) = -0.3$ dB.

The sum of the measured noise variances $(\Delta|i_+|)^2 + (\Delta|i_-|)^2$ is shown in fig. 6, together with the quantum noise limit (QNL) of the sum of the amplitude and phase quadratures of the beams which is given by $2(\Delta|i_{12}|)^2$ for coherent state beams. We see that the sum of the noise powers is below the QNL which represents an experimental demonstration of non-separability of the two beams. The degree of inseparability is close to the theoretical prediction at low frequencies and falls at high frequency which we attribute to a roll-off in the detector response.

In principle short wavelength entanglement could also be produced by mixing independently generated squeezed beams on a beamsplitter (a quantitative theoretical comparison of these approaches was given in ref. [13]). The method demonstrated here has the advantage of a considerably simpler implementation, since only one nonlinear cavity is needed, and the beams exiting the cavity are entangled without control of the relative phase of independently squeezed beams on a beamsplitter. Another approach which is comparable in complexity to that we have used is simply to divide a squeezed beam on a 50/50 beamsplitter. In such a case the degree of entanglement is $V_{\rm bs} = \frac{1}{2}(1 + S_X)$, where S_X is the amplitude quadrature noise spectrum of the beam which is divided. We compare $V_{\rm bs}$ with V of the two-port resonator in fig. 7. We see that for moderate levels of squeezing the two-port resonator produces larger entanglement. Only for strong amplitude squeezing greater than about $-6\,$dB does division on a beamsplitter produce more entanglement than is possible with the two-port resonator. As such strong squeezing has never been observed in SHG the two-port resonator method appears to be a useful alternative for creating moderate levels of entanglement. This technique

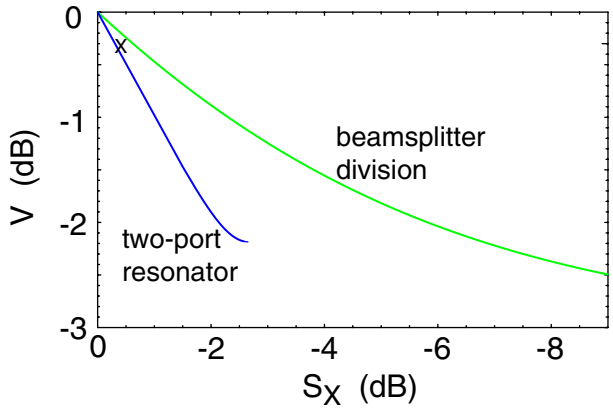

Fig. 7: (Color online) Comparison of the entanglement produced in the two-port resonator with division of a single squeezed beam on a 50/50 beamsplitter as a function of the squeezing level S_X. The results for the two-port resonator were calculated using the theory of ref. [13] with parameters corresponding to the experiments reported here. The maximum possible squeezing for the experimental resonator parameters used is about -2.7 dB. The cross shows the experimentally observed squeezing and entanglement.

may also be of particular interest for applications such as quantum lithography [3] that will benefit from short wavelength entanglement, and could also be a convenient source of tunable entanglement at atomic transition frequencies in the visible and near infrared part of the spectrum if a longer wavelength infrared pump laser is used.

In conclusion, we have demonstrated a new approach to generating bright entangled beams using SHG in a cavity with two output ports. The amount of entanglement observed was limited by the available pump power. Calculations show that $(\Delta|i_+|)^2 + (\Delta|i_-|)^2 \sim 2.4$ should be possible using available nonlinear materials with $P_{\rm pump} \sim 0.5$ W. Our calculations also predict EPR entanglement to be present at pump powers above about 50 mW (see fig. 8 in [13]). In contradistinction to previous experiments we demonstrate entanglement at a shorter wavelength than that of the pump laser.

Finally, we point out that the output beams of fig. 1 are entangled even though each beam is generated in separate $\chi^{(2)}$ interactions (they are produced by intracavity pump beams propagating in opposite directions) and they never directly interfere with each other. Thus we have demonstrated that pairwise independent nonlinear coupling of two field modes to a common shared pump mode is sufficient to generate entanglement. This type of coupling has been predicted [20] to be useful for generating tripartite entanglement between three different wavelengths and our work may be seen as a step in that direction.

* * *

This work was supported by NSF grant ECS-0533472.

REFERENCES

[1] Drummond P. D. and Ficek Z., *Quantum Squeezing* (Springer, Berlin) 2004.
[2] Polzik E. S., Carri J. and Kimble H. J., *Phys. Rev. Lett.*, **68** (1992) 3020; Schiller S., Bruckmeier R., Schalke M., Schneider K. and Mlynek J., *Europhys. Lett.*, **36** (1996) 361; Ribeiro P. H. S., Schwob C., Maître A. and Fabre C., *Opt. Lett.*, **22** (1997) 1893; Treps N., Grosse N., Bowen W. P., Fabre C., Bachor H.-A. and Lam P. K., *Science*, **301** (2003) 940.
[3] Boto A. N., Kok P., Abrams D. S., Braunstein S. L., Williams C. P. and Dowling J. P., *Phys. Rev. Lett.*, **85** (2000) 2733.
[4] Braunstein S. L. and van Loock P., *Rev. Mod. Phys.*, **77** (2005) 513.
[5] Ou Z. Y., Pereira S. F., Kimble H. J. and Peng K. C., *Phys. Rev. Lett.*, **68** (1992) 3663.
[6] Kwiat P. G., Mattle K., Weinfurter H., Zeilinger A., Sergienko A. V. and Shih Y., *Phys. Rev. Lett.*, **75** (1995) 4337.
[7] Pereira S. F., Xiao M., Kimble H. J. and Hall J. L., *Phys. Rev. A*, **38** (1988) 4931; Sizmann A., Horowicz R. J., Wagner G. and Leuchs G., *Opt. Commun.*, **80** (1990) 138; Paschotta R., Collett M., Kürz P., Feidler K., Bachor H.-A. and Mlynek J., *Phys. Rev. Lett.*, **72** (1994) 3807.
[8] Horowicz R. J., *Europhys. Lett.*, **10** (1989) 537; Dance M., Collett M. J. and Walls D. F., *Phys. Rev. A*, **48** (1993) 1532; Wiseman H. M., Taubman M. S. and Bachor H.-A., *Phys. Rev. A*, **51** (1995) 3227; Olsen M. K. and Horowicz R. J., *Opt. Commun.*, **168** (1999) 135.
[9] Olsen M. K., *Phys. Rev. A*, **70** (2004) 035801; Grosse N. B., Bowen W. P., McKenzie K. and Lam P. K., *Phys. Rev. Lett.*, **96** (2006) 063601.
[10] Andersen U. L. and Buchhave P., *J. Opt. B: Quantum Semiclass. Opt.*, **5** (2003) S486; *J. Opt. Soc. Am. B*, **20** (2003) 1947.
[11] Lodahl P. and Saffman M., *Opt. Lett.*, **27** (2002) 110; **27** (2002) 551(E); Bache M., Scotto P., Zambrini R., Miguel M. S. and Saffman M., *Phys. Rev. A*, **66** (2002) 013809.
[12] Lodahl P., *Phys. Rev. A*, **68** (2003) 023806.
[13] Lim O.-K. and Saffman M., *Phys. Rev. A*, **74** (2006) 023816.
[14] Furusawa A., Sørensen J. L., Braunstein S. L., Fuchs C. A., Kimble H. J. and Polzik E. S., *Science*, **282** (1998) 706.
[15] Duan L. M., Giedke G., Cirac J. I. and Zoller P., *Phys. Rev. Lett.*, **84** (2000) 2722.
[16] Glöckl O., Andersen U. L. and Leuchs G., *Phys. Rev. A*, **73** (2006) 012306.
[17] Korolkova N., Silberhorn C., Glöckl O., Lorenz S., Marquardt C. and Leuchs G., *Eur. Phys. J. D*, **18** (2002) 229.
[18] Drever R. W. P., Hall J. L., Kowalski F. V., Hough J., Ford G. M., Munley A. J. and Ward H., *Appl. Phys. B*, **31** (1983) 97.
[19] Bache M., Lodahl P., Mamaev A. V., Marcus M. and Saffman M., *Phys. Rev. A*, **65** (2002) 033811.
[20] Olsen M. K. and Bradley A. S., *Phys. Rev. A*, **74** (2006) 063809.